An optofluidic device for characterizing the effect of viscosity and density on mass transfer

Michael Ian Lapsley[*], Nitesh Nama [*], Shahrzad Yazdi[**] and Tony Jun Huang[*]

[*]Department of Engineering Science and Mechanics, [**]Department of Mechanical Engineering, The Pennsylvania State University, University Park, PA 16802, USA, junhuang@psu.edu

ABSTRACT

We introduce a device which can monitor the diffusion of highly concentrated aqueous solutions. In our study, we analyze the effects of viscosity on the mass transfer process in this device. Two mathematical models are used to interpret concentration data at the sidewall of the channel, acquired via optofluidic means. In addition, optical images record the viscosity induced interface shift. All of the results are compared by analyzing the interface shift they produce in the system and we verify that this interface shift is cause by differences in viscosity through COMSOL simulations. We plan to extend this work to produce a compact device to measure the diffusion coefficients of highly concentrated solutions.

Keywords: Microfluidics, Optofluidics, Diffusion, Viscosity, Mass Transfer

1 INTRODUCTION

Diffusion is an important phenomena in the fields of biochemistry, [1], [2] food science, [3] pharmaceuticals [4] and optofluidics. [5] Several studies have emerged to analyze the physics of mass transfer in microfluidic channels; however, these studies usually rely on fluorescent tags which are viewed using fluorescent microscopes. [6–9] This is not convenient for non-fluorescent samples as fluorescent tags can alter the mass transfer rates of small molecules and some substances may not have the option of using fluorescent tags (such as salt solutions). In addition, much of the previous work uses low concentrations (or low concentration differences) of samples to force the mass transfer to take place only through diffusion. At high concentrations, effects due to viscosity and density can play a major role in mass transfer. The diffusion of $CaCl_2$ at high concentrations is of great interest especially in optofluidic devices. Recently, the effects of viscosity on mass transfer between two miscible fluids was analyzed. [10] In this study, we introduce a simple device used to analyze the diffusion of high concentration of calcium chloride ($CaCl_2$).

2 DIFFUSION THEORY

2.1 Reaction Model

It has been shown that simple diffusion of a single species can be modeled as a chemical reaction. [11] The mass balance for such a system is:

$$V_D \frac{dC}{dt_D} = A_D j_D \tag{1}$$

Where C is the concentration of the species, V_D is the volume into which the species is diffusing, t_D is the time over which the diffusion takes place, A_D is the area across which the diffusion takes place. And j_D is the flux of the species into the volume. The flux into the system is defined by the reaction relationship and Eqn. 1 is rewritten as:

$$V_D \frac{dC}{dt_D} = A_D \frac{D}{l}\left[C_{SAT} - C\right] \tag{2}$$

Where D is the diffusivity, C_{SAT} is the saturation concentration and l is the diffusion length. Solving this single ordinary differential equation yields:

$$C = C_{SAT}\left(1 - e^{(aD)(t_D - b)}\right) \tag{3}$$

$$a = \frac{A_D}{V_D l} \tag{4}$$

For our system (Fig. 1a) the flow rate can be converted to "diffusion time (t_D)" by considering the detection point (L), the flow rate (Q) and the cross-sectional area of the channel (A_C):

$$t_D = \frac{LA_C}{Q} \tag{5}$$

This model is useful because of its simplicity; however, many physical parameters contribute to the values of a and b. Thus, it was difficult to connect physical parameters directly with these coefficients.

2.2 Mass Transport Model

Our system (Fig. 1a and Fig. 5a) can be more accurately modeled using the concepts of mass transport in the conservation of mass equation:

$$\frac{\partial C}{\partial t}+\vec{U}\bullet\nabla C = D\nabla^2 C \tag{6}$$

$$\frac{\partial C}{\partial t}+u\frac{\partial C}{\partial x}+v\frac{\partial C}{\partial y}+w\frac{\partial C}{\partial z}=D\left(\frac{\partial^2 C}{\partial x^2}+\frac{\partial^2 C}{\partial y^2}+\frac{\partial^2 C}{\partial z^2}\right) \tag{7}$$

where U is the vector velocity (with x, y and z components noted as u, v, and w). In our device, we assume: the system is steady state; there is no velocity in the y and z direction; and diffusion takes place only in the y direction. Based on these assumptions, Eqn. 7 reduces to:

$$u(y,z)\frac{\partial C}{\partial x}=D\frac{\partial^2 C}{\partial y^2} \tag{8}$$

where u is the velocity in the x direction. Due to the parabolic velocity distribution in microfluidic channels, u is a function of y and z which complicates Eqn. 8. To simplify the model, the variation of u in the z and y directions is ignored.

The boundary conditions use to solve Eqn. 8 were:

$$\frac{\partial C}{\partial y}(x,0)=\frac{\partial C}{\partial y}(x,w_c)=0 \tag{9}$$

$$C(0,y)=\begin{cases}0 & , \quad y<0\\ C_0 & , \quad 0<y<s\\ 0 & , \quad s<y\end{cases} \tag{10}$$

$$C(\infty,y)\neq\infty \tag{11}$$

Where w_c is the width of the channel, and s is the position of the interface between the two fluids. Assuming that u is a constant, a simple analytical solution can be reached:

$$C(x,y)=\frac{C_0 s}{w}+\sum_{n=1}^{N=\infty}A_n\cos\left(\frac{n\pi}{w}y\right)e^{-\lambda_n x} \tag{12}$$

$$\lambda_n=\left(\frac{n\pi}{w}\right)^2\frac{D}{u} \tag{13}$$

$$A_n=\frac{2C_0}{n\pi}\sin\left(\frac{n\pi h}{w}\right) \tag{14}$$

3 EXPERIMENT

A schematic of the device is shown in Fig. 1a. A single microfluidic channel with two inlets and one outlet was fabricated in polydimethylsiloxane (PDMS). The width (w_c) and height of the channel were 400 and 125 µm, respectively. Water is injected into one inlet and solutions of Calcium Chloride ($CaCl_2$) in the other.

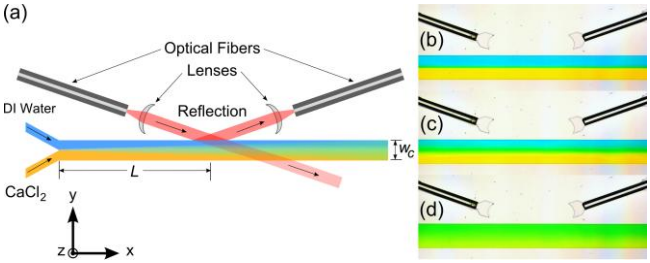

Figure 1: (a) Schematic of the device. (b-d) Experimental images of diffusion at several flow rates.

Guide channels were fabricated to align two optical fibers on the water side of the microfluidic channel, as shown in Fig. 1a. PDMS-air lenses were fabricated at the end of the guide channels to collimate the incident beam emitted from the input fiber and couple the reflected beam to the output fiber. Optical images of the device shown in Fig.1 b-d illustrate the alignment of the optical fibers and the position of the collimating lenses. Laser light from an argon ion laser, having a wavelength of 532 nm, was coupled to the input optical fiber and projected to the water side of the microfluidic channel as seen in Fig. 1 a. The refractive index difference between the PDMS sidewall and the fluid caused part of the light to be reflected, and the remainder was transmitted. The refractive index is proportional to concentration as discussed in our previous work. [12] The output optical fiber collects the reflected light and guides it to an optical power meter. The analog output of the optical power meter was connected to an oscilloscope to collect data. For each test, 10,000 data points were recorded over a period of 40 seconds to record the variance in the signal. This system allows the concentration near the sidewall of the channel to be monitored.

4 RESULTS AND DISCUSSION

Two experimental images in Fig. 2 indicate that the interface between the two fluid streams shifts at high concentrations of $CaCl_2$. Initially, the main mechanism causing the shift was unclear. Two-dimensional, simulations were run in COMSOL to determine the cause of the shifts, and the results are shown in Fig. 3. In Fig. 3a, the viscosity was held constant and equal to water while the density increased with concentration linearly. A small shift was observed at the inlet, but the interface quickly returns

to the center of the channel. In Fig. 3b, the density was held equal that of water and the viscosity varied linearly with concentration. A large shift was observed at high concentrations of $CaCl_2$ and the shift remained throughout the length of the channel.

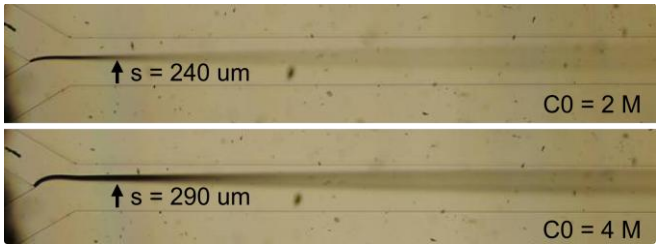

Figure 2: Experimental images of the shift in the interface between the two fluids.

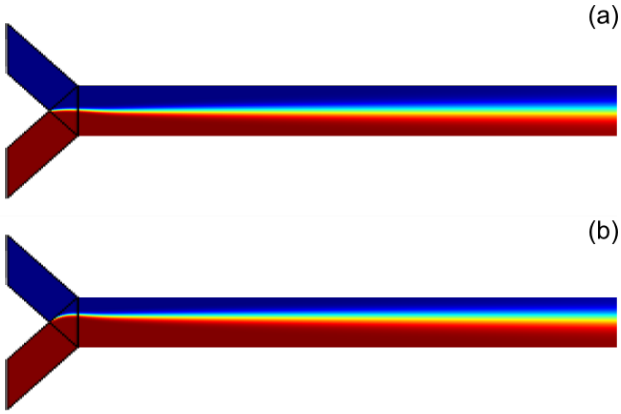

Figure 3: (a) COMSOL simulation results for a test varying only density with concentration. (b) COMSOL simulation results for a test varying only density with concentration.

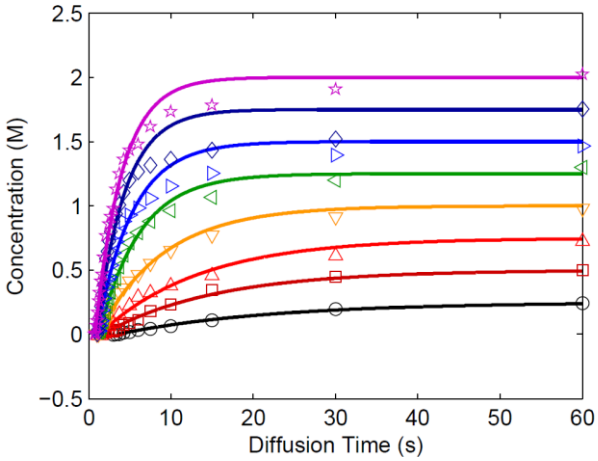

Figure 4: Reflection data for concentration with flow rate converted to time fitted with the results from the reaction model.

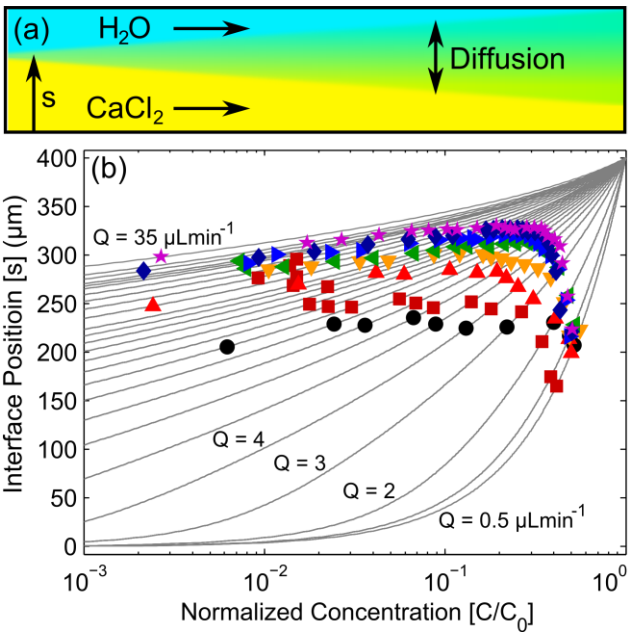

Figure 5: Experimental data fit to the results of mass transfer model.

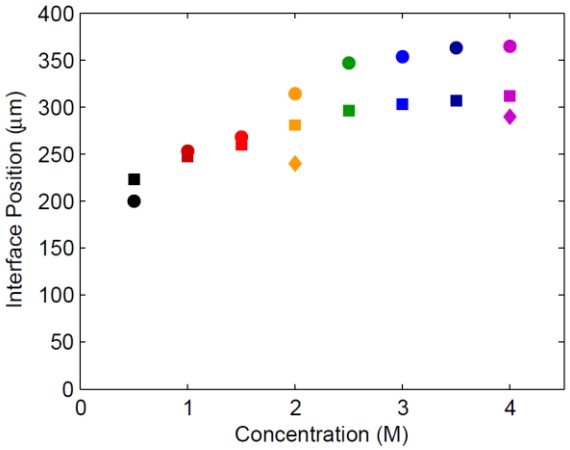

Figure 6: Comparison of all the results. Circle: concentration data via reaction model; Square: concentration data via mass transfer model; Diamond: results from experimental images.

The concentration data and the experimental images can be compared by considering the effect of the interface shift. The two models discussed in the theoretical section allow the interface shift to be predicted based on the concentration recorded. Several initial concentrations (from 0.5 to 4 M) were loaded in the $CaCl_2$ channel and the concentrations were measured at flow rates from 0.5 to 30 µL/min. The flow rate was converted to t_D by Eqn. 5, and the data was plotted in Fig. 4. The reaction model, described by Eqns. 3-5, was fit with the results and these fits are shown as solid lines in Fig. 4. The coefficients a and b in Eqn. 3 were determined using the least squares method

for each concentration. The interface shift (*s*) was determined assuming that *l* is the length from the interface to the sidewall where concentration is measured, thus:

$$s = w_c - l \tag{16}$$

The ratios, A_D/V_D, for each concentration were determined using Eqn. 4, assuming that *l* at *C* = 0.5 M was 200 µm. The same data was analyzed using the mass transfer model described by Eqns. 12-14. Interface shift vs concentration calculated by this model at each flow rate of interest was plotted as the gray lines in Fig. 5b, and the experimental data was fit to these lines. Finally, the predicted interface position for each model and those from the experimental images are plotted in Figure 6. We see that the trend for each analysis is similar. Thus, the viscosity difference between the two fluids effects both the interface position and the concentration at the sidewall, and this effect is predictable. The mass transfer model gives a closer approximation of the concentration data, as expected. The inaccuracy in the reaction model can be attributed to the uncertainty in determining A_D and V_D. Through further development, this system could be used to measure the diffusion coefficients of unknown solutions, allowing us to use diffusivity as a label-free sensing parameter.

5 CONCLUSION

We have shown that an optofluidic setup can be used to detect the concentration at the side wall of a fluid channel and monitor the diffusion in the system. Through our analysis, we see the effects of viscosity on the diffusion characteristics. This study mainly provides a fundamental understand of how viscosity affects the mass transfer in a microchannel. The next step is to fully characterize the system to produce a miniaturized system which can determine the diffusion characteristics of biomolecules for diagnosis and characterization purposes.

REFERENCES

[1] R. R. Walters, J. F. Graham, R. M. Moore, and D. J. Anderson, "Protein diffusion coefficient measurements by laminar flow analysis: Method and applications," *Analytical Biochemistry*, vol. 140, no. 1, pp. 190-195, Jul. 1984.

[2] D. Brune and S. Kim, "Predicting protein diffusion coefficients," *Proceedings of the National Academy of Sciences of the United States of America*, vol. 90, no. 9, pp. 3835-3839, May 1993.

[3] E. Demirkol, F. Erdogdu, and T. K. Palazoglu, "Analysis of mass transfer parameters (changes in mass flux, diffusion coefficient and mass transfer coefficient) during baking of cookies," *Journal of Food Engineering*, vol. 72, no. 4, pp. 364-371, 2006.

[4] A. W. Larhed, P. Artursson, J. Grasjo, and E. Bjork, "Diffusion of drugs in native and purified gastrointestinal mucus," *J. Pharm. Sci.*, vol. 86, no. 6, pp. 660-665, 1997.

[5] X. Mao, S.-C. S. Lin, M. I. Lapsley, J. Shi, B. K. Juluri, and T. J. Huang, "Tunable Liquid Gradient Refractive Index (L-GRIN) lens with two degrees of freedom.," *Lab on a Chip*, vol. 9, no. 14, pp. 2050-2058, 2009.

[6] A. E. Kamholz, E. A. Schilling, and P. Yager, "Optical Measurement of Transverse Molecular Diffusion in a Microchannel," *Biophysical Journal*, vol. 80, no. 4, pp. 1967-1972, 2001.

[7] J. Kim and Y. S. Ju, "On-chip characterization of the mass diffusivity of binary mixtures using Brownian microscopy," *Sensors and Actuators A: Physical*, vol. 155, no. 1, pp. 39-46, 2009.

[8] R. F. Ismagilov, A. D. Stroock, P. J. A. Kenis, G. Whitesides, and H. A. Stone, "Experimental and theoretical scaling laws for transverse diffusive broadening in two-phase laminar flows in microchannels," *Applied Physics Letters*, vol. 76, no. 17, pp. 2376-2378, Apr. 2000.

[9] D. Broboana, C. Mihai Balan, T. Wohland, and C. Balan, "Investigations of the unsteady diffusion process in microchannels," *Chemical Engineering Science*, vol. 66, no. 9, pp. 1962-1972, May 2011.

[10] J. Dambrine, B. Géraud, and J.-B. Salmon, "Interdiffusion of liquids of different viscosities in a microchannel," *New Journal of Physics*, vol. 11, no. 7, p. 75015, 2009.

[11] E. L. Cussler, *Diffusion: Mass transfer in fluid systems*. Cambridge University Press, 2009.

[12] M. I. Lapsley, S.-C. S. Lin, X. Mao, and T. J. Huang, "An in-plane, variable optical attenuator using a fluid-based tunable reflective interface," *Applied Physics Letters*, vol. 95, no. 8, p. 083507, 2009.